Analysis of hysteretic behavior in a FeCoB-based nanocrystalline alloy by a Preisach distribution and electron holography

Jianguo Long,[a] M. E. McHenry, and D. E. Laughlin
Department of Material Science and Engineering, Carnegie Mellon University, Pittsburgh, Pennsylvania 15213, USA

C. Zheng, H. Kirmse, and W. Neumann
Institut für Physik, Humboldt-Universität zu Berlin, D-12489 Berlin, Germany

(Presented on 6 November 2007; received 10 September 2007; accepted 3 October 2007; published online 24 January 2008)

First order reverse curves have been used to investigate the Preisach distribution and electron holography to observe the spatial variation of the magnetization in $Fe_{40}Co_{40}Nb_4B_{13}Ge_2Cu_1$ nanocomposite alloys after annealing at 500, 550, 610, and 960 °C for 1 h. Grain sizes observed for these annealing temperatures varied from 10 to 200 nm. The Preisach distribution reveals that the magnetization process in the sample annealed at 500 °C for 1 h was dominated by reversible processes, consistent with a small coercivity and mobile domain walls in an external field. At higher annealing temperatures, the irreversible magnetization processes became dominant with increasing grain size. Electron holography observations of the domains show that, for the sample annealed at 500 °C, the magnetic flux distribution was uniform with few pinning barriers to domain wall motion consistent with reversible magnetization. The sample annealed at 610 °C exhibited irregularity in the shape of magnetic flux lines attributed to the inhomogeneous magnetization distribution due to the α-FeCo and $(FeCoNb)_{23}B_6$ phases present after secondary crystallization. © *2008 American Institute of Physics*. [DOI: 10.1063/1.2829395]

I. INTRODUCTION

Nanocomposite materials are promising candidates for power conversion applications due to their excellent soft magnetic properties.[1–4] The attractive soft magnetic properties derive from the two phase microstructure consisting of ferromagnetic grains surrounded by a ferromagnetic amorphous matrix. The amorphous precursors produced by melt spinning are generally annealed above their primary crystallization temperature to obtain the optimal microstructure and soft magnetic properties. After crystallization, nanocrystals are typically 10 nm in average size. Since the grain size of the nanocrystalline phases is much smaller than the magnetic exchange length, the magnetocrystalline anisotropy and magnetostriction coefficient are averaged over the many small grains (called random magnetic anisotropy).[5–7] Thus, soft magnetic properties are improved through the suppression of the effective K by grain refinement.

The Preisach model[8,9] considers a system comprised of a collection of elementary nonsymmetric hysteresis loops, each characterized by its up and down switching fields. The probability density describing the distribution of elementary loops in the collection fully characterizes the system. The Preisach model is widely studied and employed as a mathematical tool for the treatment of hysteretic phenomena.

The first order reversal curve (FORC) can be used to reconstruct the Preisach distribution from experimental data.[10] The measurement of a FORC begins by saturating a sample in a large positive magnetic field. Subsequently, the field is reduced to a field h_a, and the FORC is determined as the magnetization curve (M-h curve) when the applied field is increased from h_a back to saturation. By measuring a series of M-h curves for different values of h_a, one obtains a family of curves. The magnetization at the arbitrary applied field h_b, which is between h_a and the saturation field, is denoted by $M(h_a,h_b)$, where $h_b > h_a$. The Preisach distribution is defined as the mixed second derivative:

$$\rho(h_a,h_b) = -\frac{\partial^2 M(h_a,h_b)}{\partial h_a \partial h_b},$$

where $\rho(h_a,h_b)$ is well defined for $h_b > h_a$.

In this paper, we use FORCs to calculate the Preisach distribution and apply the Preisach model to analyze the hysteretic behavior and to compare the results with the spatial dispersion of magnetic flux density determined by electron holography for a nanocrystalline FeCoB-based soft magnetic alloy.

II. EXPERIMENTAL

An amorphous ribbon with a thickness of ~30 μm and nominal composition $Fe_{40}Co_{40}Nb_4B_{13}Ge_2Cu_1$ was prepared by a single roller melt spinning. An alloy ingot prepared by arc melting was then induction melted in a quartz crucible and cast in argon onto a copper wheel rotating at ~50 m/s in a vacuum chamber. Amorphous ribbon samples were subsequently crystallized by sealing them in evacuated silica tubes, placing them in a preheated furnace at prescribed temperatures, and finally quenching them in water at room tem-

[a]Electronic mail: jianguol@andrew.cmu.edu

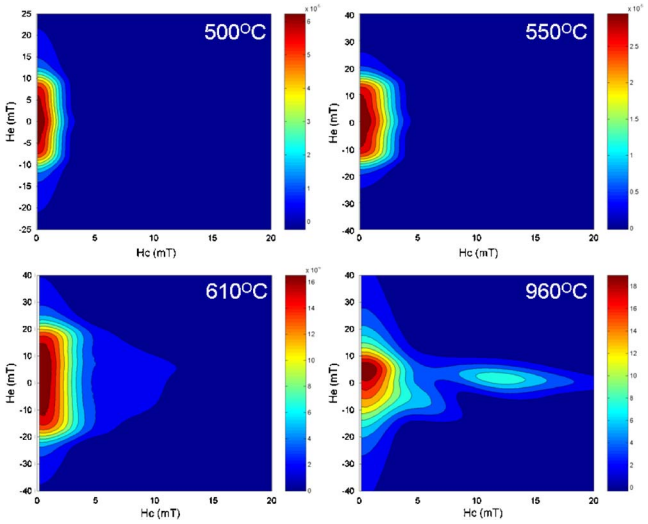

FIG. 1. (Color online) Contour plots of the Preisach distribution calculated from FORCs of the sample annealed at 500, 550, 610, and 960 °C.

perature. The annealing temperatures were 500, 550, 610, and 960 °C and the annealing time is 1 h for all cases.

An alternating gradient-force magnetometer was used to measure the FORC data for these annealed samples. The transmission electron microscopy (TEM) and electron holography investigations were carried out with a JEOL JEM-2200FS transmission electron microscope. This microscope is equipped with a field emission gun, an electrostatic biprism, and an objective minilens. Both the Lorentz microscopy and electron holography were carried out in a low magnification mode. In this mode, the objective lens is switched off and the electron beam is focused by an objective minilens so that the samples are located in a field-free environment. Plane view TEM samples were used for the electron holography observations.

III. RESULTS AND DISCUSSION

Figure 1 shows the distribution $\rho(h_c,h_e)$ contour plot of the samples annealed at selected temperatures, reconstructed from a series of first order reverse curves. For the purpose of plotting the FORC distribution, it is convenient to change the coordinates from (h_a,h_b) to $(h_c=(h_a-h_b)/2,\ h_e=(h_a+h_b)/2)$. The magnetizations of the FORCs were normalized by the saturation magnetization before calculating the distribution. A legend for the contour shadings is shown at the right of the diagram. In our previous works,[11,12] the average grain size of annealed samples was determined to be ~10 nm for 500 °C, ~18 nm for 550 °C, ~90 nm for 610 °C, and >200 nm for 960 °C. Figures 1(a)–1(d) show the Preisach distribution of the samples annealed at these temperatures. The maximum distribution value for samples annealed at 500, 550, and 610 °C is located at $h_c=0$ and $h_e=0$, while for the sample annealed at 960 °C, above its second crystallization temperature, there is an irreversible peak located at about $h_c=12$ mT. With increasing annealing temperature, the contours are observed to be more spread out horizontally.

The Preisach distribution can be subdivided into two parts: $\rho(h_c,h_e)=\rho_{\mathrm{rev}}(h_e)+\rho_{\mathrm{irr}}(h_c,h_e)$. $\rho_{\mathrm{rev}}(h_e)$ represents the reversible distribution (the distribution along the $h_c=0$ line of the Preisach plane) describing the reversible process, such as wall bowing inside potential wells and coherent magnetization rotations inside domains; $\rho_{\mathrm{irr}}(h_c,h_e)$ represents the irreversible process which describes the irreversible domain wall jumps, such as Barkhausen jumps. To compare these contour plots of distribution under different annealing temperatures, the higher the annealing temperature, the more the irreversible process is inside the sample. For a better look at the distribution changing with annealing temperature, we plot a vertical cross section through $h_c=0$ in Fig. 2 and a horizontal cross section at $h_e=0$ in Fig. 3.

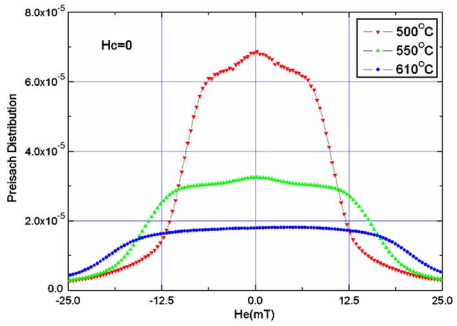

FIG. 2. (Color online) The distribution profile plot of $\rho(h_c=0,h_e)$ along the $h_c=0$ line.

Figure 2 shows the $\rho(h_c=0,h_e)$ distribution profile, which describes the reversible process. The distribution is most dispersed in the small h_e region for the sample annealed at 500 °C, which comprised of ~10 nm α-FeCo nanoparticles embedded in an amorphous matrix. These nanoparticles, surrounded by an amorphous matrix, can be regarded as isolated from each other. With increasing annealing temperature, the average grain size increases further and the particles come in contact with each other and their interaction becomes strong. The distribution is spread out over a larger h_e region for the sample annealed at 610 °C, as shown in Fig. 2.

The basic Preisach model assumes a Gaussian distribution of interaction fields; however, the observation suggests that well isolated particles in the sample annealed at 500 °C produce the narrow Gaussian distribution and large particles or clusters in the sample annealed at 610 °C, in which there is a strong but localized interaction, produces the wider Gaussian distribution. Figure 3 shows the distribution profile

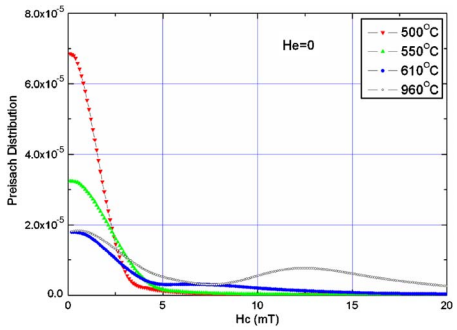

FIG. 3. (Color online) The distribution profile plot of $\rho(h_c,h_e=0)$ along the $h_e=0$ line.

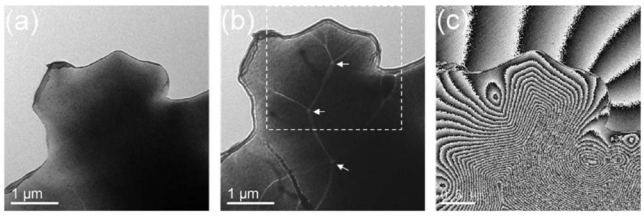

FIG. 4. [(a) and (b)] Lorentz image and (c) electron holography image of the square region in (b) for the sample annealed at 500 °C. Arrows in (b) indicate the pinning sites.

along the $h_e=0$ line which should correspond to the irreversible magnetic process. The distribution sharply dropped from the peak value to zero for the sample annealed at 500 °C. This indicates that the reversible process is dominant in this sample. For higher annealing temperature, an irreversible peak is observed located at $h_c=8$ mT for the sample annealed at 610 °C and $h_c=12$ mT for 960 °C.

TEM confirms that the sample annealed at 500 °C for 1 h consisted of fine particles (α-FeCo) with an average particle size of 10 nm in an amorphous matrix. These fine particles grow further to ~90 nm after anneal at 610 °C for 1 h. There is little residual amorphous phase in the sample annealed at 610 °C. Both Lorentz microscopy and electron holography show that few pinning sites and larger magnetic domain are observed in the sample annealed at 500 °C, as shown in Figs. 4. Figure 4 shows Lorentz mode domain observations and an electron holography image for an $Fe_{40}Co_{40}Nb_4B_{13}Ge_2Cu_1$ alloy annealed at 500 °C for 1 h. The magnetization distribution is shown in the reconstructed phase image of Fig. 4(b) obtained from electron holography. The shape of magnetic flux lines changes smoothly.

Figure 5 illustrates the Lorentz mode image and phase image of domain configuration of the sample annealed at 610 °C for 1 h. The black and white lines in the Lorentz image indicate the domain wall. This figure shows the size of the magnetic domains to become smaller and the shape of the lines of magnetic flux to become more irregular. The irregularity in the shape of the lines of magnetic flux is attributed to the inhomogeneous magnetization distribution due to the difference in magnetization of the α-FeCo and the FeCo-B compounds. In the sample annealed at 610 °C, domain walls are only observed to reside in the intergranular regions and domains include several grains. In combination with the Preisach analysis, this indicates that the irreversible portion of the hysteretic response in the sample annealed at 610 °C corresponds to a population of pinning sites located at the intergranular regions and the large grain size.

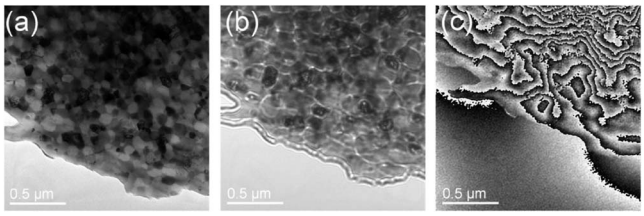

FIG. 5. [(a) and (b)] Lorentz image and (c) electron holography image of the sample annealed at 610 °C.

IV. CONCLUSION

We used the FORC data of a nanocrystalline soft magnetic $Fe_{40}Co_{40}Nb_4B_{13}Ge_2Cu_1$ alloy to calculate the Preisach distribution based on the Preisach model. The Preisach distribution shows that the reversible magnetic process is dominant in the annealed sample when the grain size is small. With grain size increased by annealing the alloy at higher temperature, irreversible magnetic processes become dominant and give rise to magnetic hardening. This is ascribed to pinning sites in the intergranular regions as evident by irregularity of magnetic flux line revealed by electron holography.

ACKNOWLEDGMENTS

This work was supported by the National Science Foundation (DMR-0406220). This work was also supported in part by the Army Research Laboratory and was accomplished under Cooperative Agreement No. W911NF-04-2-0017.

[1] Y. Yoshizawa, S. Oguma, and K. Yamauchi, J. Appl. Phys. **64**, 6044 (1988).
[2] K. Suzuki, A. Makino, A. Inoue, and T. Masumoto, J. Appl. Phys. **70**, 6232 (1991).
[3] M. A. Willard, D. E. Laughlin, M. E. McHenry, D. Thoma, K. Sickafus, J. O. Cross, and V. G. Harris, J. Appl. Phys. **84**, 6773 (1998).
[4] M. A. Willard, M.-Q. Huang, D. E. Laughlin, M. E. McHenry, J. O. Cross, V. G. Harris, and C. Franchetti, J. Appl. Phys. **85**, 4421 (1999).
[5] G. Herzer, IEEE Trans. Magn. **26**, 1397 (1990).
[6] G. Herzer, J. Magn. Magn. Mater. **112**, 258 (1992).
[7] G. Herzer, Scr. Metall. Mater. **33**, 1741 (1995).
[8] I. D. Mayergoyz, *Mathematical Models of Hysteresis* (Springer-Verlag, New York, 1991).
[9] F. Preisach, Z. Phys. **94**, 277 (1935).
[10] C. R. Pike, A. P. Roberts, and K. L. Verosub, J. Appl. Phys. **85**, 6660 (1999).
[11] J. Long, Y. Qin, T. Nuhfer, M. De Graef, D. E. Laughlin, and M. E. McHenry., J. Appl. Phys. **101**, 09N115 (2007).
[12] J. Long, P. R. Ohodnicki, D. E. Laughlin, M. E. McHenry, T. Ohkubo, and K. Hono, J. Appl. Phys. **101**, 09N114 (2007).